

Method for Detecting Weld Feature Size Based on Line Structured Light

ZHU Huayu¹, LU Yonghua^{1*}, LI Yanlong², TAN Jie², FENG Qiang²

1. College of Mechanical and Electrical Engineering, Nanjing University of Aeronautics and Astronautics, Nanjing 210016, P.R. China; 2. State-Owned Jinjiang Machine Factory, Chengdu 610043, P.R. China

(Received 29 March 2021; revised 24 May 2021; accepted 30 May 2021)

Abstract: With the rapid development of the machining and manufacturing industry, welding has been widely used in forming connections of structural parts. At present, manual methods are often used for welding and quality inspection, with low efficiency and unstable product quality. Due to the requirements of visual inspection of weld feature size, a visual inspection system for weld feature size based on line structured light (LSL) is designed and built in this paper. An adaptive light stripe sub-pixel center extraction algorithm and a feature point extraction algorithm for welding light stripe are proposed. The experiment results show that the detection error of the weld width is 0.216 mm, the detection error of the remaining height is 0.035 mm, the single measurement costs 109 ms, and the inspection stability and repeatability of the system is 1%. Our approach can meet the online detection requirements of practical applications.

Key words: optical inspection; weld; feature size; light stripe center extraction; feature point extraction

CLC number: TP391 **Document code:** A **Article ID:** 1005-1120(2021)03-0383-10

0 Introduction

Welding is commonly used as combination metals or other thermoplastic materials, thanks to its high connection strength and high reliability. Nowadays, with the rapid development of machining and manufacturing, it has been widely used in forming connections of structural parts. The quality of welding determines the quality of the product and its service life to a great extent. At present, in most manufacturing companies in China, the welding and welding seam grinding processes mainly adopt manual methods: Depending on human eyes to judge whether the characteristic size of the welding seam is reasonable, and whether there are defects such as welding knobs, pores or cracks, as well as to determine the quality of the weldment. However, the manual detection is inefficient and has the disadvantages of missing detection and misjudgment. The manual grinding seriously affects the product quality with

low production efficiency, and sometimes even the metal base material is damaged because of poor accuracy and low efficiency. Therefore, improving the efficiency of welding operations and the quality of welding products is critical to modern welding production.

The active visual inspection technology based on structured light has the advantages of high accuracy, fast measurement speed, and good anti-interference. It has become a hot spot in recent years, and been applied to the high-precision inspection process of parts^[1-3]. The optical measurement method is based on modern optical technology and combines multi-disciplinary technologies such as optoelectronics, computer vision, and graphics. Thanks to its simpler structure, high detection efficiency and accurate measurement, it has become the first choice of optical measurement, and been rapidly developed. It is widely used in the field of dimensional measurement, three-dimensional topography reconstruc-

*Corresponding author, E-mail address: nuaa_lyh@nuaa.edu.cn.

How to cite this article: ZHU Huayu, LU Yonghua, LI Yanlong, et al. Method for detecting weld feature size based on line structured light[J]. Transactions of Nanjing University of Aeronautics and Astronautics, 2021, 38(3): 383-392.

<http://dx.doi.org/10.16356/j.1005-1120.2021.03.003>

tion, and surface quality inspection.

The structured light measurement method can meet the requirements of high accuracy, high stability and high real-time performance of welding seam detection. Accurately obtaining the remaining dimensions of the welding seam after the welding is the key factor to effectively repair the welding seam and improve the grinding quality of the weld^[4]. Therefore, in this paper, a three-dimensional visual measurement method based on line structured light is proposed to position weld feature points and to detect geometric feature sizes.

1 Design of Visual Inspection System for Welds

The visual inspection system designed in this paper aims to realize the automatic measurement of the weld geometry. The detection system and the geometric quantity to be measured are shown in Fig.1. The geometric quantity means the width and the remaining height of the weld. The system developed in this paper needs to ensure high measurement accuracy and stability in real-time while measuring geometric dimensions.

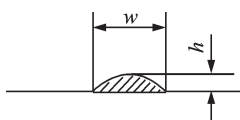


Fig.1 Detection system and geometric quantity to be measured

A typical weld generally consists of a weld zone, a fusion line, a heat-affected zone, and its parent material, as shown in Fig.2(a). The geometrical parameters of the weld are shown in Fig.2(b). Due to the practical situations and the difficulty of visual measurement, the system only measures the weld width and the remaining height. The detection error of the weld width must be within 0.25 mm and the detection error of the remaining height must be within 0.10 mm.

The vision detection system consists of a laser projection module and an image acquisition module. We choose the laser tilt and camera vertical layout,

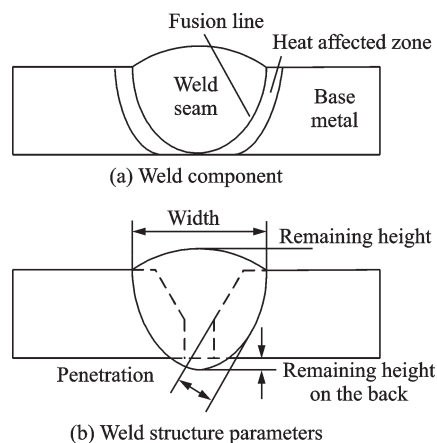


Fig.2 Components and structural parameters of a weld

which is easy to realize. The structure is simple, and the welding seam is enlarged.

The hardware platform of the visual inspection system for weld feature size based on line structured light is shown in Fig.3. It is mainly composed of a line structured light sensor, a fixture module, a detection object, a stepper motor, and an optical experiment bench.

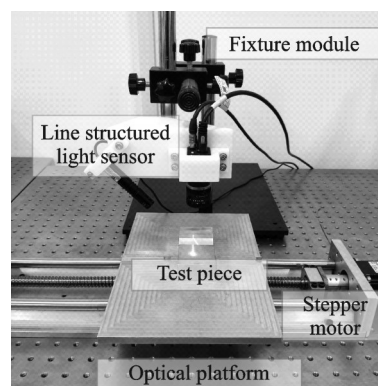


Fig.3 Hardware platform of the visual detection system

2 Line Structured Light Stripe Center Extraction Algorithm

Since the actual light stripe has a certain width, the center line of the light stripe must be extracted first in the implementation process of the 3D visual measurement technology based on line structured light. Therefore, the accuracy of extracting the center of the light stripe is very important to the performance of the entire system and directly affects the measurement accuracy. Based on the investigation of line structure light stripe characteristics, influenc-

ing factors of center extraction and its principle, this paper proposes an adaptive optimization algorithm, and conducts detailed experimental verification, multi-dimensional algorithm evaluation and result analysis.

Due to the influence of external environmental factors, the vibration of the device during operation, and the hardware of the system itself, noise often exists in the light stripe image acquired by the sensor. In order to reduce the influence of noise and improve the signal-to-noise ratio of the image, median filtering is used to denoise the original image. Then, the maximum inter-class variance method is used to segment the light stripe image, and the binarized light stripe is well extracted to ensure the accurate extraction of subsequent light stripe centers. The image preprocessing results are shown in Fig.4.

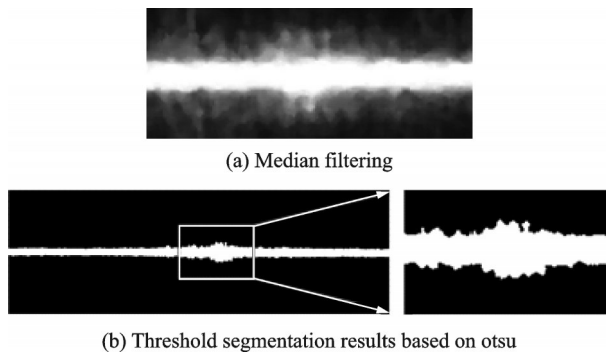


Fig.4 Image preprocessing results

The traditional line structured light stripe center extraction algorithm is divided into two aspects: extracting the geometric center, and extracting energy center of the light stripe. The former mainly includes the geometric center method, the threshold method and the skeleton refinement method^[5]. These algorithms are fast to extract, but less accurate. The latter mainly includes the directional template method, the gray center of gravity method, the Steger method, and the curve fitting method^[6-8]. The directional template method has poor stability, and the accuracy of its center extraction is average. Based on the principle of the gray barycenter method, this paper proposes a robust adaptive center extraction algorithm for the case that the width of each cross section of the actual light stripe is different and

there are multiple gray levels^[9-10].

(1) Detecting the boundary of the light stripe

Pixels are retrieved column by column from the two ends of the binarized light stripe image to the middle. When the gray value $f(x, y) = 255$ is detected for the first time on the left end or the pixel gray value $f(x, y) = 255$ is detected for the last time in a column on the right, scanning detection is stopped. The pixels obtained at this time are recorded as P_l and P_r , and their coordinates are (x_l, y_l) and (x_r, y_r) . The set of pixels in the target area of the light stripe can be expressed as

$$\{f(x, y) | x_l \leq x \leq x_r, y_l \leq y \leq y_r\} \quad (1)$$

Since the width of the light stripe varies in the length direction, this paper detects the upper and the lower boundaries of the light stripe in the target area to obtain the width of each section, and adaptively extracts the center point within this range. The pixel set $f_i(x, y)$ of the i th section of the light stripe that participates in the calculation of the center point is

$$\begin{aligned} & \{f_i(x, y) | y_{up}(i) \leq y(i) \leq y_{down}(i)\} \text{ or} \\ & \{f_i(x, y) | y_{up}(i) \leq y(i) \leq y_{up}(i) + w_i\} \end{aligned} \quad (2)$$

where $f_i(x, y)$ represents the pixel point with coordinates (x, y) on the i th section, $i = x + 1$; $y_{up}(i)$ and $y_{down}(i)$ are the vertical coordinates of the upper and the lower boundaries of the i th light stripe section, respectively; w_i is the width of each section, $w_i = y_{down}(i) - y_{up}(i)$.

(2) Adaptive light strip sub-pixel center extraction

The difference in pixel gray value at the center of the stripe is small, which is a grayscale characteristic of the actual light stripe. At the same time, the gray-center-of-gravity method is susceptible to noise. In this paper, the quadratic weighted center of the gravity method based on the adaptive width is used to extract the center point P of each section. The calculation principle of this method is shown in Fig.5. This method uses the pixel information in the adaptive width range and increases the gray value of the central area of the light stripe to calculate the weight. The solid green dots in the figure are the extracted sub-pixel center points.

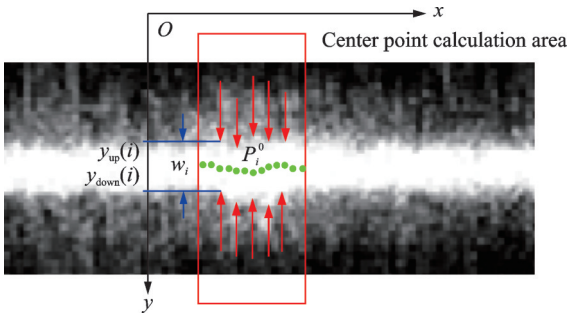


Fig.5 Schematic diagram of the quadratic weighted bary-center method based on the adaptive width

Convolution calculations have low efficiency and insufficient stability in the normal direction of each point. And the research objects in this section are horizontal light streaks. There is no need to consider their directivity. Only the ordinate $y_{\text{center}}^0(i)$ of the center point of the i th section needs to be calculated. Then the point $P_i^0(x, y_{\text{center}}^0(i))$ is the extracted initial center point (where $x = i - 1$). $y_{\text{center}}^0(i)$ is calculated as

$$y_{\text{center}}^0(i) = \frac{\sum_{y=y_{\text{up}}(i)}^{y_{\text{up}}(i)+w_i} f_i(x, y)^2 \cdot y}{\sum_{y=y_{\text{up}}(i)}^{y_{\text{up}}(i)+w_i} f_i(x, y)^2} \quad (3)$$

(3) Optimal relocation based on center point discrete analysis

In order to further improve the accuracy of center point extraction and reduce the impact of background noise, this paper analyzes the initial center point P_i^0 to optimize its relocation. Then it uses the least square method to perform center point fitting. The final subpixel light strip center is obtained.

Suppose a window with a length of a , the center of the window is set as the initial center point of each section, and moves from left to right according to the light stripe section. Every time a section is moved, the average y -coordinate of the initial center point in the window is calculated to obtain the optimized center point $P_i^1(x, y_{\text{center}}^1(i))$

$$y_{\text{center}}^1(i) = \frac{\sum_{m=i-\frac{a-1}{2}}^{i+\frac{a+1}{2}} y_{\text{center}}^0(m) - y_{\text{center}}^0(i)}{a-1} \quad (4)$$

where i and m represent the serial number of the light stripe section; $y_{\text{center}}^0(i)$ and $y_{\text{center}}^0(m)$ the coordinates

of the initial center point of the i th and the m th sections, respectively; point P_i^0 is the center of the current optimization window; a the calculation window size, which is usually an odd number ($a \geq 1$).

According to the light strip boundary points P_l and P_r obtained in the previous section, calculate the slope threshold k_T is calculated to evaluate the dispersion of the initial center point

$$k_T = \frac{y_r - y_l}{x_r - x_l} \quad (5)$$

Then the center point P_i^1 is traversed after the average optimization according to the length of the light stripe, and the slope k_1 between the current center point P_i^1 and the $(i-b)$ th section center point P_{i-b}^1 is calculated

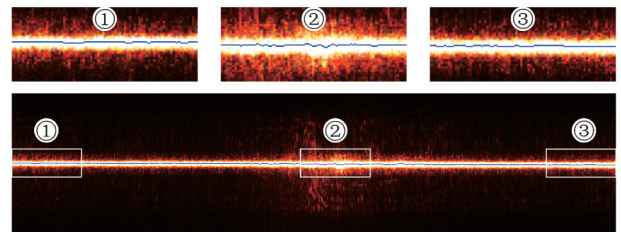
$$k_1 = \frac{y_{\text{center}}^1(i) - y_{\text{center}}^1(i-b)}{i - (i-b)} \quad (6)$$

A dispersion analysis is conducted based on the thresholds k_T and k_1 to determine whether there is a large deviation from the initial center point. According to the analysis of the experimental data in this paper, when k_1 is 10 times more than k_T , it is considered that there is a large deviation in the center point P_i^1 , and it needs to be optimized and repositioned. Taking the $(i-b)$ th section center point P_{i-b}^1 as the reference point for relocation, the calculation formula is as follows

$$y_{\text{center}}^2(i) = \begin{cases} y_{\text{center}}^1(i) & k_1 \leq 10k_T \\ y_{\text{center}}^1(i-b) + b \times k_T & k_1 > 10k_T \end{cases} \quad (7)$$

The sub-pixel coordinate of the center point P_i^2 obtained through the above two optimization steps is $(x, y_{\text{center}}^2(i))$.

Fig.6 is the result of extracting the center point of the light stripe by the optimization algorithm. Fig.7 shows the comparison between the extraction



①—③: Three details extracted from the center of the light bar

Fig.6 Light strip center extraction results of the proposed optimization algorithm

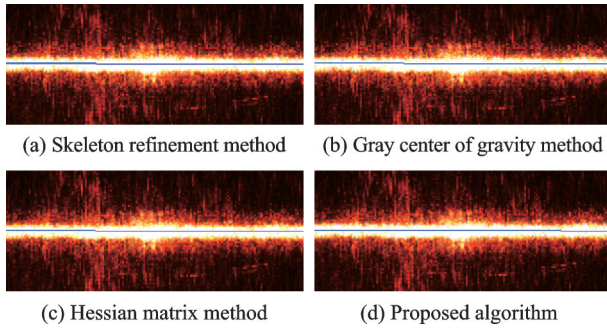


Fig.7 Light strip center extraction results of the four algorithms

results of the three traditional algorithms and the proposed optimization algorithm. It can be seen from Fig.7 that macroscopically, the lines fitted by the above four algorithms are almost all located at the actual center of the light stripe. There is little difference between them. The position of the center line is relatively accurate.

The standard deviation of the distance from the center point of the light strip to the fitted straight line extracted by the algorithm is used to characterize the accuracy. A small standard deviation value indicates that the extracted center point is less discrete and the algorithm performs at a higher precision. On the contrary, it means that the algorithm center point extraction is unstable.

The calculation formula of the standard deviation of the distance from the center point to the fitted straight line extracted by the algorithm is

$$\sigma = \sqrt{\frac{\sum_{i=1}^n (d_i - \bar{d})^2}{n}} \quad (8)$$

where d_i the distance from the i th center point to the fitted straight line; \bar{d} the average of the distances from each center point to the fitted straight line; and n the number of center points extracted.

d_i is calculated according to the distance formula from a point to a straight line

$$d_i = \left| \frac{ax_i + by_i + c}{\sqrt{a^2 + b^2}} \right| \quad (9)$$

where (x_i, y_i) is the center point of the i -th light stripe; a, b, c are the coefficients of the linear equation $ax + by + c = 0$ for the fitted light stripe.

The accuracy level, the running time t , and the standard deviation σ of each algorithm are shown

in Table 1. It can be seen that, compared with the three algorithms, the proposed algorithm presents an obviously better extraction effect. The position of the center point is accurate and stable. The fitted centerline is also fully able to characterize the actual appearance of light streaks.

Table 1 Accuracy analysis of different algorithms

Performance	Skeleton refinement method	Gray center of gravity method	Hessian matrix method	The proposed algorithm
Accuracy level	Pixel	Sub-pixel	Sub-pixel	Sub-pixel
t/ms	642	32	811	31
$\sigma/pixel$	0.32	0.55	0.28	0.23

3 Image Processing and Feature Point Extraction Algorithm for Welding Light Stripe

After the in-depth study of the stripe center extraction algorithm, the next step is to perform image preprocessing on the weld stripe image. Based on the recognition of the light stripe type and with the center extraction optimization algorithm proposed in this paper, the feature points are accurately extracted to obtain the actual geometric feature size of the weld.

There are fewer feature points to be extracted in the light stripe image of the weld. Feature points can be directly extracted after image preprocessing. Image preprocessing generally includes region of interest (ROI) extraction, image filtering and threshold segmentation. Combined with the system parameters, the characteristic size of the weld can be output^[11]. The general steps are shown in Fig.8.

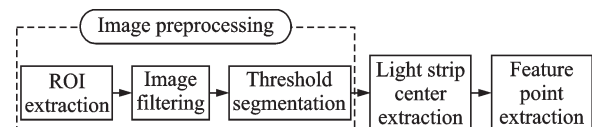


Fig.8 Flow chart of welding stripe image processing and feature point extraction algorithm

It is difficult to guarantee higher welding quality during the welding process. Welds may have defects such as pits, pores, and incomplete penetration. As a result, the geometric characteristics of

the sections of the actual weld are different, and they are not all arc-shaped. Therefore, the algorithm of extracting weld feature points should also be able to adapt to different situations. That is, the characteristic points of the welding seam light stripe with accurate geometric shapes can be accurately extracted.

(1) Multi-type seam light strip image segmentation

The camera captures multiple weld seam images with different cross sections. The four most representative light stripe images were selected as the objects. The obtained light stripe images of the weld are shown in Fig.9. The quality of the weld shown in Fig.9 (a) is the best. The modulated light stripe appears as an arc and feature points are easy to extract. The weld quality in Fig.9 (b) is the second. The light stripe is roughly two arcs. The welds shown in Fig.9 (c, d) have obvious welding defects. The quality of them is poor, the characteristics of the light stripe are not obvious, and the features are hard to point positioned.

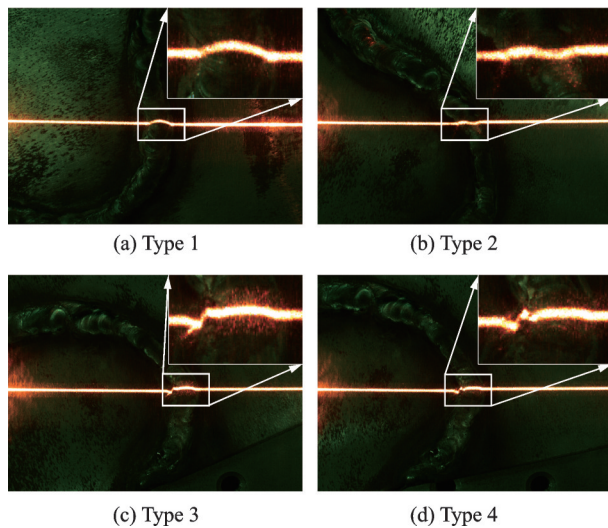


Fig.9 Light stripe images of different types of welds

Next, the images of the light stripe of the weld were preprocessed. Since the gray level difference between the light strip area and the background in the image was obvious, it is easy to segment the light stripes. The image pre-processing algorithm of the light stripe image used in this paper is shown in Fig.10.

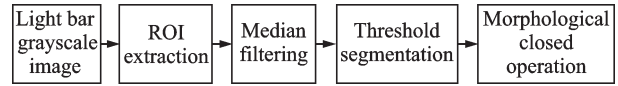


Fig.10 Image preprocessing algorithm for weld light stripe

Median filtering was used to remove pepper, salt, and solitary point noise. The images were binarized by the Otsu method. Since the edge of the binarized light stripe after threshold segmentation looked like terraced, a morphological closed operation was used to smooth the light stripe edge^[12-13]. The final processing results are shown in Fig.11. The light stripe target of the weld is accurately extracted. The implementation of the preprocessing algorithm works well.



Fig.11 Images of binarized weld light stripe

(2) Extraction algorithm of weld feature points based on the two-parameter threshold

After the image preprocessing, the sub-pixel center point of the light stripe of the weld seam was extracted using the adaptive center extraction optimization algorithm mentioned above. The center points were stored in the point set $Weld_crtP$ ^[14-15]. Since efficiency is particularly important in the automated inspection of weld quality, we directly extracted the feature points of the light stripe of the weld based on the central point set $Weld_crtP$.

The welding light stripe was divided into three parts S_1 , S_2 , and S_3 , as shown in Fig.12. The characteristic points W_L and W_R of the weld zone are the start and the end positions of the weld. The characteristic point W_D is the lowest point of the weld. The characteristic point W_U is the highest points of the weld. Through the extraction of these four fea-

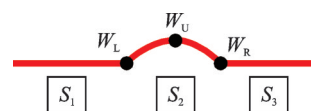


Fig.12 Division of light stripe area of weld

ture points, the width and the remaining height of the weld can be calculated and obtained.

By analyzing the morphological characteristics of the light stripe of the weld in the image, the feature points were extracted into two parts: The start and the end feature points W_L and W_R of the weld seam, and the feature height points W_D and W_U . In this paper, the two-parameter threshold method was used to extract the characteristic points W_L and W_R of the weld. The specific implementation steps of the algorithm are as follows.

Step 1 The moving rectangular window W in the initialization image is set with a size of $2a+1$, and the center of the window is placed at the $a+1$ sub-pixel center point of the extracted light stripe. The window with a $W_{\text{size}}=3$ is shown in Fig.13.

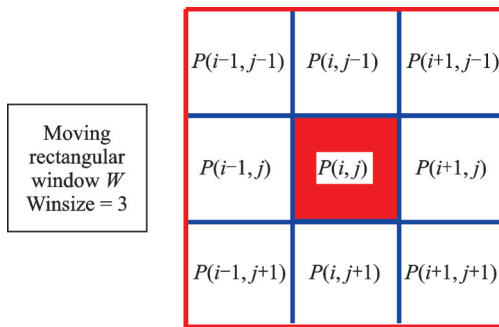


Fig.13 Moving rectangular window for feature point extraction of welds

Step 2 Calculate the average slopes \bar{k}_l and \bar{k}_r of the light stripes on both sides of the window center, and the average ordinates \bar{y}_l and \bar{y}_r .

Step 3 Calculate the average slope difference $\Delta\bar{k}$ and the average ordinate difference $\Delta\bar{y}$ on both sides of the rectangular window center.

Step 4 Based on the slope threshold $k_{w,T}$ and the ordinate threshold $y_{w,T}$, the magnitudes between the average slope difference $\Delta\bar{k}$ and the average ordinate difference $\Delta\bar{y}$ are compared. Determine whether the center point of the rectangular window is the feature point of the light stripe to be extracted. If $\Delta\bar{k}$ and $\Delta\bar{y}$ are greater than the thresholds $k_{w,T}$ and $y_{w,T}$ at the same time, the window stops moving. The detected feature point W_L (W_R) is output. If not, the window moves one pixel from left to

right (right to left) and returns to Step 2.

The results of the extraction of weld feature points are shown in Fig.14. The solid dots are the extracted feature points. It can be seen that although the types of welds are different, the required toe and height feature points in them can be accurately extracted.

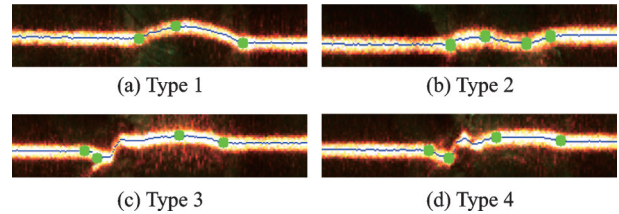


Fig.14 Feature point extraction results of the light stripe of the weld

4 Analysis of Test Results

After the software function of the visual inspection system is realized. A detection test was performed on the weld object constructed in this paper to analyze the accuracy of the core algorithm of the system and the detection performance of the entire system.

The high-precision measuring equipment selected was an absolute measuring arm of Hexagon, and its contact measurement accuracy was ± 0.051 mm. The measurement results of the system in this paper were compared with the real values obtained by the measurement arm, and the detection performance of the accuracy, stability, and repeatability errors of the constructed system was tested and analyzed.

In order to effectively evaluate the accuracy of the geometric measurement of the weld in this paper, two approximate straight lines of the weld sample were selected, as shown in the wire frame in Fig.15(a), and Fig.15(b) is the geometric quantity to be measured of the weld: width w , remaining height h . The linear motion and image acquisition parameters of the system were readjusted, the light stripe images were acquired in real time, and the measurement results were output. In this paper, a total of 60 sets of geometric data of the weld section were obtained.

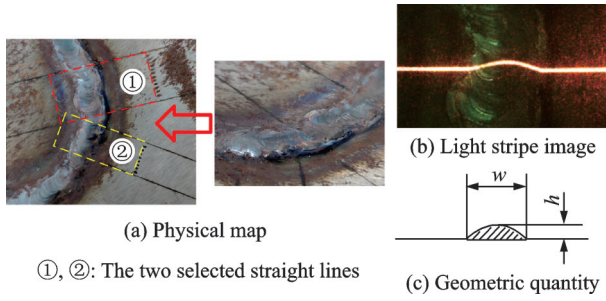


Fig.15 Weld sample and its measured geometry

The actual dimensions of the weld geometric quantities w and h and the system measurement results in this paper are shown in Table 2. The average absolute measurement error of the geometric quantity w is 0.216 mm, and the geometric quantity h is 0.035 mm. Both were within the range of the system measurement error index.

Table 2 Accuracy test results of weld feature size measurement

Geometric quantity	Actual value	Measurements	Mean absolute error
w/mm	6.127	5.937	0.216
	6.308	6.134	
	6.223	6.027	
	⋮	⋮	
	6.130	5.920	
	5.781	5.465	
h/mm	0.702	0.726	0.035
	0.751	0.780	
	0.776	0.784	
	⋮	⋮	
	0.756	0.804	

In order to clearly show the distributions of the measured value and the true value of each sampling section, the true and the measured value graphs drawn according to the data in Table 1 are shown in Fig.16. Fig.16(a) shows the weld width w , and Fig.16(b) shows the remaining height h of the weld. It can be seen that the change trend of the system measurement results in this paper is basically consistent with the real value, that is, it can accurately reflect the actual morphological change of the test piece. Specifically, in Fig.16(a), the measured values of the weld width of each section are smaller than their true values. The main reason is that the height of the weld to be tested is low and the gradi-

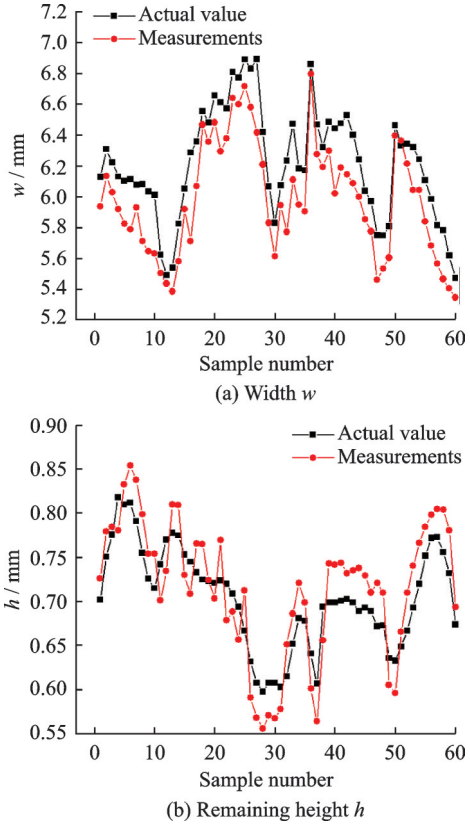


Fig.16 Distribution curves of true values and measured values of weld geometry

ent of the boundary area between the two welded plates is small, which makes the algorithm have a certain deviation when extracting the feature points of the weld width and shortens the distance inward.

In Fig.16(b), the measured values of the residual height in each section of the system are larger or smaller than the true values. Since the residual height is less than 1 mm, this change may be caused by the relative position of the height feature points. It may be caused by the uncertainty when artificially selecting the height detection point to calculate the true value.

However, it can be obtained from the absolute error distribution chart in Fig.17 that the absolute deviation of w fluctuates within the range of 0.1—0.3 mm, and the average error is 0.216 mm. It does not obviously cause deviation in feature point extraction. The measurement error of the remaining height h is in the range of 0.025—0.045 mm, and the average error is 0.035 mm. It indicates that the measurement of the remaining height is accurate and stable, and meets the actual detection requirements.

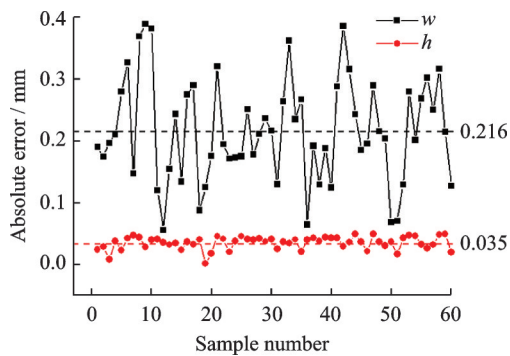


Fig.17 Absolute error distribution of weld feature size measurement

5 Conclusions

In order to meet the needs of visual inspection of the geometric characteristics of weld seams, this paper proposes a 3D visual inspection approach based on line structured light, and combines structural design, image processing and software development technologies to design and implement a visual inspection system of weld geometric dimensions. The test results showed that the detection error of weld width was 0.216 mm, the detection error of remaining height was 0.035 mm, and the maximum processing time of a single image was only 109 ms, which has reached the system development goal of this subject. Some conclusions can be drawn.

(1) This paper proposed an adaptive light strip sub-pixel center extraction algorithm and multi-dimensional accuracy evaluation indexes. They can effectively solve the uneven light strip width and gray distribution non-uniform problems with high extraction accuracy, good real-time performance, and good robustness.

(2) For different types of weld images, a differential image preprocessing method based on the ROI region division is used to effectively filter out the background noise of the light strip image and accurately extract the light strip target.

(3) A fusion algorithm of type recognition and corner location is proposed. The corners are initially located while recognizing the type of image, and the center of the light stripe is extracted to obtain the sub-pixel feature points of the weld. The algorithm achieves fast and accurate feature point extraction.

References

- [1] VAZQUEZ M A, CUEVAS F J. A 3D facial recognition system using structured light projection[C]//Proceedings of International Conference on Hybrid Artificial Intelligence Systems. Salamanca, Spain: Springer International Publishing, 2014: 241-253.
- [2] YU Haotian, HUANG Yu, ZHENG Dongliang, et al. Three-dimensional shape measurement technique for large-scale objects based on line structured light combined with industrial robot[J]. *Optik*, 2020, 202: 163656.
- [3] MEI Junhua, LAI Leijie. Development of a novel line structured light measurement instrument for complex manufactured parts[J]. *The Review of Scientific Instruments*, 2019, 90(11): 115106.
- [4] SHAO J X, DU D, CHANG B H, et al. Automatic weld defect detection based on potential defect tracking in real-time radiographic image sequence[J]. *NDT & E International*, 2012, 46: 14-21.
- [5] LI Y H, ZHOU J B, HUANG F S, et al. An improved gray weighted method for sub-pixel center extraction of structured light stripe[C]//Proceedings of International Conference on Sensing Technology. Nanjing, China: IEEE, 2016.
- [6] CHEN X Z, WANG X C, CAO Y, et al. Color structure-light stripe center-line extraction method research[C]//Proceedings of the 34th Chinese Control Conference. Hangzhou, China: IEEE, 2015.
- [7] KWON J H, IM S B, CHANG M H, et al. A digital approach to dynamic jaw tracking using a target tracking system and a structured-light three-dimensional scanner[J]. *J Prosthodont Res*, 2019, 63 (1) : 115-119.
- [8] PARK J, KIM C, NA J, et al. Using structured light for efficient depth edge detection[J]. *Image and Vision Computing*, 2008, 26(11): 1449-1465.
- [9] LU Yonghua, ZHANG Jia, LI Xiaoyan, et al. A robust method for adaptive center extraction of linear structured light stripe[J]. *Transactions of Nanjing University of Aeronautics and Astronautics*, 2020, 37(4) : 586-596.
- [10] PPTER F, DUVIEUBOURG L, MACAIRE L. Fast laser stripe extraction for 3D metallic object measurement[C]//Proceedings of IECON 2016—42nd Annual Conference of the IEEE Industrial Electronics Society. Florence, Italy: IEEE, 2016.
- [11] XU Y L, YU H W, ZHONG J Y, et al. Real-time seam tracking control technology during welding robot GTAW process based on passive vision sensor[J]. *Journal of Materials Processing Technology*, 2012,

212(8): 1654-1662.

- [12] STARK J A. Adaptive image contrast enhancement using generalizations of histogram equalization[J]. IEEE Transactions on Image Processing, 2000, 9(5): 889-896.
- [13] HU B, LI D H, JIN G, et al. New method for obtaining the center of the structured light stripe by direction template[J]. Computer Engineering & Applications, 2002, 38(11): 59-60, 109.
- [14] SENGEE N, SENGEE A, CHOI H. Image contrast enhancement using bi-histogram equalization with neighborhood metrics[J]. IEEE Transactions on Consumer Electronics, 2010, 56(4): 2727-2734.
- [15] YE Z, PEI Y, SHI J. An improved algorithm for harris corner detection[C]//Proceedings of the 2nd International Congress on Image and Signal Processing. Tianjin, China: IEEE, 2009.

Acknowledgements This work was supported by the National Natural Science Foundation of China (No. 51975293) and the Aeronautical Science Foundation of China (No. 2019ZD052010).

Authors Mr. ZHU Huayu is a postgraduate student at

Nanjing University of Aeronautics and Astronautics. His main research is focused on machine vision and deep learning.

Prof. LU Yonghua received his Ph. D. degree in mechatronic engineering from Nanjing University of Aeronautics and Astronautics, China, in 2005. He is currently a professor at the College of Mechanical and Electrical Engineering, Nanjing University of Aeronautics and Astronautics. His research interests include intelligent detection and control, test systems, robots, and sensors.

Author contributions Mr. ZHU Huayu completed the overall design of the weld seam visual inspection system, designed and completed the linear structured light stripe center extraction algorithm and feature point extraction algorithm. Prof. LU Yonghua helped to verify the feasibility and reliability of the detection method. Mr. TAN Jie and Mr. LI Yanlong completed the collection of weld seam images. Mr. FENG Qiang helped to complete the experimental data analysis. All authors commented on the manuscript draft and approved the submission.

Competing interests The authors declare no competing interests.

(Production Editor: ZHANG Bei)

基于线结构光的焊缝特征尺寸检测方法

朱华煜¹, 陆永华¹, 李雁龙², 谭杰², 冯强²

(1. 南京航空航天大学机电学院, 南京 210016, 中国; 2. 国营锦江机械厂, 成都 610043, 中国)

摘要: 随着机械加工与制造行业的迅速发展, 焊接已被广泛运用于结构件的成型连接中。目前多采用人工方式进行焊接和焊缝质量检测, 生产效率低下, 产品质量不稳定。本文针对焊缝特征尺寸视觉检测需求, 以焊缝为研究对象, 搭建了基于线结构光的焊缝特征尺寸视觉检测系统, 提出了一种自适应的光条亚像素中心提取算法和一种焊缝光条的特征点提取算法。实验结果表明: 焊缝宽度的检测误差为 0.216 mm, 焊缝余高的检测误差为 0.035 mm, 单次测量在 109 ms 内, 系统的检测稳定性和重复性为 1%, 满足了实际应用的在线检测要求。

关键词: 光学检测; 焊缝; 特征尺寸; 光条中心提取; 特征点提取